北見工業大学研究報告
第18巻 第2号 (昭和62年)

Memoirs of the Kitami Institute of Technology
Vol. 18 No. 2 (1987)

Characterization of Surface Oxygen Species on Zinc Oxide Revealed by the ESR Technique and the Transient Response Method*

by Takuma KIMURA**, Tohru KANNO***, Masatoshi HAYASHI**** and Masayoshi KOBAYASHI***

Department of Industrial Chemistry, Kitami Institute of Technology, 090 Kitami, Hokkaido, Japan

(Received October 1, 1986)

Abstract

The nature and reactivity of the oxygen species adsorbed on zinc oxide have been studied in detail over the temperature range room temperature-230°C by using the ESR technique, the transient response method and an electrical conductivity measurement of the catalyst. The results obtained from the dynamic procedures have simultaneously suggested that there are three different kinds of oxygen species (O_2^-, O^- and O (non-ionic form)) on the surface during reaction. O_2^- is assigned by the ESR technique using the g-values $g_{xx}=2.0499$, $g_{yy}=2.0030$ and $g_{zz}=2.0093$, and it exists stably on the surface below 190°C. It disappears easily on exposure to CO, suggesting an induced charge transfer from O_2^- to the catalyst.

The existence of O^- and O is predicted by the transient behaviour of gaseous O_2 and electrical conductivity, and the two species commonly react with CO apparently obeying first order kinetics. The mode of the transient response curves of the CO_2 formed shows a typical type VI curve based on the classification of the mode of response curves. From this result, it is presumed that the reaction consists of two different paths: one is the reaction of gaseous CO and O^- and the other is the reaction of CO and O. The apparent activation energy is 104 kJ/mol for the over-all reaction.

1. Introduction

In 1974, Tanaka and Blyholder[1~4] clearly demonstrated that oxygen species adsorbed on ZnO are classified as O_2^-, O^- and O_3^-, and O_2^- is extremely inactive for CO oxidation and $^{16}O_2$–$^{18}O_2$ exchange reaction. O_3^- is an intermediate formed by the reaction of O_2 with O^-, and is thought to be unstable. The reactivity of nonionic oxygen species (expressed as O(a)) has not been discussed enough since Amigures and Teichner[5] and Sancier[6] twenty years ago.

In our previous papers[7,8], we showed by using the KI-method and the electrical conductivity measurement of a catalyst, that O_2^- adsorbed on MnO_2 is as

* The paper was partly presented at the Hokkaido regional meeting of the Chemical Society of Japan in the winter period of 1980.

** Chemical Environmental Engineering.

*** Department of Industrial Chemistry.

**** Makkari Village Office.

reactive for CO oxidation as the coexisting O^- species.[7] Furthermore, on silver supported on α-alumina, O_2^- is more reactive than O^- for CO oxidation.[8] The nature and reactivity of oxygen species adsorbed on metals or metal oxides, thereby sensitively depend on the reaction conditions and the kind of catalysts. In the present study, the Electron Spin Resonance (ESR) technique is used to analyse O_2^- and special attention is paid to follow the dynamic behavior of O_2^-. The transient response method[9,10] is also employed to study the reactivity of the neutral oxygen species with no charge, and the electrical conductivity of the catalyst is simultaneously measured to follow the charge transfer between the adsorbed species and the catalyst.

2. Experimental Procedure

(1) Catalyst

The zinc oxide used in this study was commercially prepared by Kanto Chemical Co. The fine white powder was dried at 120°C for 3 hrs in an air flow, and the sample was then pressed by 275.5 kg/cm² for two or three minutes. It was crushed in an agate mortar and sieved so as to become 20～40 mesh. The sample was then heated in an N_2 stream for 24 hrs and then in an O_2 stream for 24 hrs at 330°C, to stabilize the catalytic activity. The impurities detected in the sample were sulfur 0.03 wt%, Pb 0.02 wt% and Fe 0.002 wt%, and the purity of ZnO was 99.2～99.3%. The BET surface area was evaluated to be 4.4 m²/g by using krypton adsorption at the temperature of liquid nitrogen.

(2) Electrical Conductivity Cell

Fig. 1 illustrates the electrical conductivity cell for the catalyst. Two round platinum plates (0.5 mm thickness and 9.7 mm diameter) were prepared as electrodes, and each had fifty pores of 0.2 mm diameter for gas flow. One Pt plate were set at each end of the catalyst bed, and 0.5 g of catalyst was mounted between the two. The plate at the top side was pressed by a stainless steel spring so as to ensure good contact with the catalyst particles. The electrical conductivity was continuously measured by the DC method as shown by Fig. 2. A standard resistor of 100 ohms was set in the loop of the conductivity circuit, and the drop of electrical voltage due to the resistor was measured by a microvolt meter (Ohkura AM-1001A). A mercury battery of 1.3 volt was stably used for the electrical power supply of the circuit.

(3) ESR Spectrum Measurement Apparatus

Fig. 3 illustrates the apparatus used to measure the ESR spectrum under *in-situ* conditions. The ESR tube is connected with a gas chamber to follow the ESR spectrum under the unsteady state conditions during exposure to O_2 or CO gas. Cock A is used to introduce the gas into the ESR tube. The main system of ESR equipment used was JEOL JEF-FE3XG as presented in Fig. 4. The temperature of the catalyst was changed by a heated air flow using JEOL ES-VT-3A.

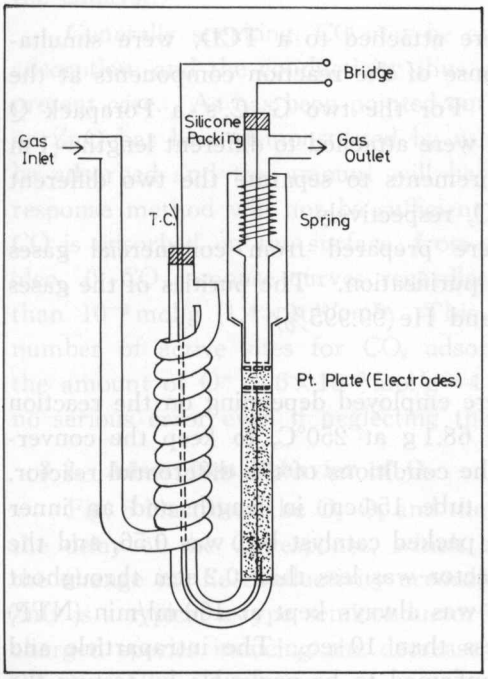

Fig. 1. Schematic drawings of the reactor equipped with a cell for measuring conductivity.

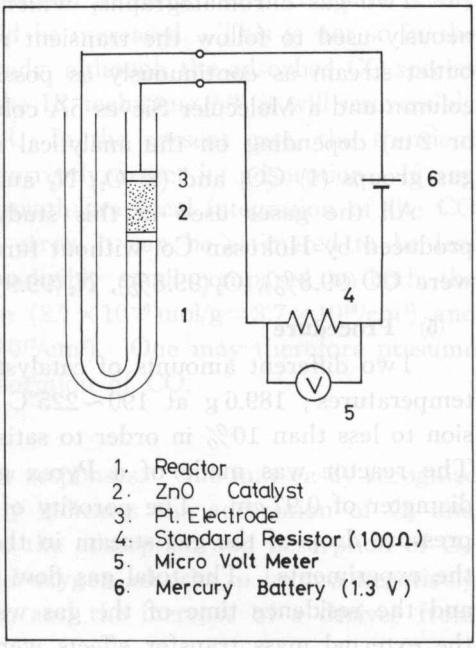

Fig. 2. DC electrical circuit to measure the conductivity of the catalyst.
A, B: vacuum cock. C: gas chamber.

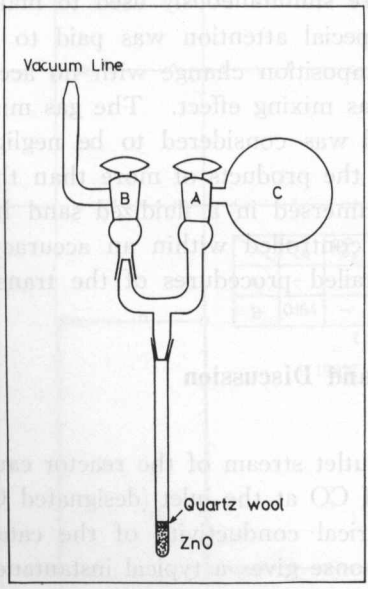

Fig. 3. The sample tube measuring the ESR spectra under the reaction conditions.

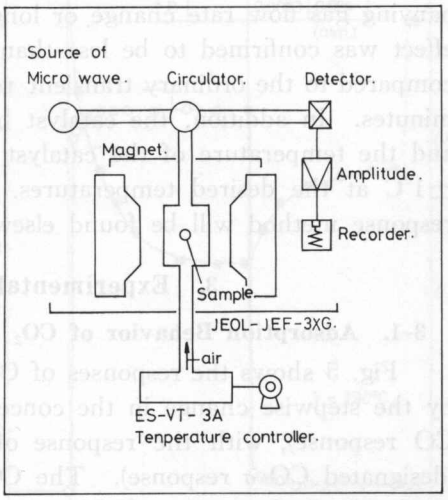

Fig. 4. Block diagram of the ESR system.

(4) Gas Analysis

Two gas chromatographs, which were attached to a TCD, were simultaneously used to follow the transient response of the reaction components at the outlet stream as continuously as possible. For the two G. C.'s, a Porapack Q column and a Moleculer Sieves 5A column were attached to different lengths (1 m or 2 m) depending on the analytical requirements to separate the two different gas groups (1) CO_2 and (2) O_2, N_2 and CO, respectively.

All the gases used in this study were prepared from commercial gases produced by Hokusan Co. without further purification. The purities of the gases were CO (99.8%), O_2 (99.8%), N_2 (99.9%) and He (99.995%).

(5) Procedure

Two different amounts of catalyst were employed depending on the reaction temperatures; 189.6 g at 190~225°C and 68.1 g at 250°C, to keep the conversion to less than 10% in order to satisfy the conditions of the differential reactor. The reactor was made of a Pyrex glass tube 154 cm in length and an inner diameter of 0.97 cm. The porosity of the packed catalyst bed was 0.56, and the pressure drop of the gas stream in the reactor was less than 0.2 atm throughout the experiments. The total gas flow rate was always kept at 160 ml/min (NTP) and the residence time of the gas was less than 10 sec. The intraparticle and the external mass transfer effects were confirmed to be negligible by testing the catalytic activity of CO oxidation, using two different sizes of catalyst particle, (20~42 and 80~100 mesh), and two different flow rates of reactant gases, (160 and 320 ml/min), under the same W/F.

Three gas flow controlling equipments were simultaneously used to make a quick stepwise change in gas composition. Special attention was paid to give the correct rectangular function to the gas composition change with no accompanying gas flow rate change or longitudinal gas mixing effect. The gas mixing effect was confirmed to be less than 5 sec, and was considered to be negligible compared to the ordinary transient response of the products of more than thirty minutes. In addition, the catalyst bed was immersed in a fluidized sand bath, and the temperature of the catalyst was well controlled within an accuracy of ±1°C at the desired temperatures. More detailed procedures of the transient response method will be found elsewhere.[8]

3. Experimental Results and Discussion

3-1. Adsorption Behavior of CO_2

Fig. 5 shows the responses of CO at the outlet stream of the reactor caused by the stepwise change in the concentration of CO at the inlet (designated CO-CO response), with the response of the electrical conductivity of the catalyst (designated CO-σ response). The CO-CO response gives a typical instantaneous mode which shows a negligible amount of adsorbed CO or no adsorption of CO on the surface.[11] In addition, the CO-σ response clearly indicates no change in the conductivity suggesting no charge transfer between the adsorbed species and

the catalyst.

Generally speaking, CO may be chemisorbed to form CO^+,[12] if there is any adsorption, and the conductivity thus should be increased. This is not so in the present case. As has been pointed out already, although the adsorbed CO species on ZnO has been demonstrated by using the IR technique,[13,14] it will irreversibly be adsorbed and the amount will be small. In the present case, the transient response method will not be sufficient to correctly detect its adsorption. If any CO is adsorbed on the surface, from the rough graphical integration of the CO (dec., 0)-CO response curves regardless of error, it can be estimated to be less than 10^{-9} mol/g (1.4×10^{10}/cm^2). This is negligibly small compared to both the number of active sites for CO_2 adsorption (2.7×10^{-6} mol/g$=3.7\times10^{13}$/cm^2) and the amount of O^- (3.6×10^{-6} mol/g$=4.9\times10^{13}$/cm^2). One may therefore presume no serious error even if neglecting the adsorption of CO.

3-2. Adsorption Behavior of O_2

Fig. 6 illustrates the O_2-O_2 and the O_2-σ responses. One may easily recognize the delay of the O_2-response, which clearly indicates the adsorption of O_2 and the change in the conductivity according to the adsorption and desorption of O_2. ZnO is a typical n-type semiconductor[12] and oxygen adsorbs to form a negatively charged species inducing the decrease of σ, and the increase of σ derives from the desorption of oxygen.

The response of O_2, when O_2 is decreased to nil (designated O_2 (dec., 0)-O_2

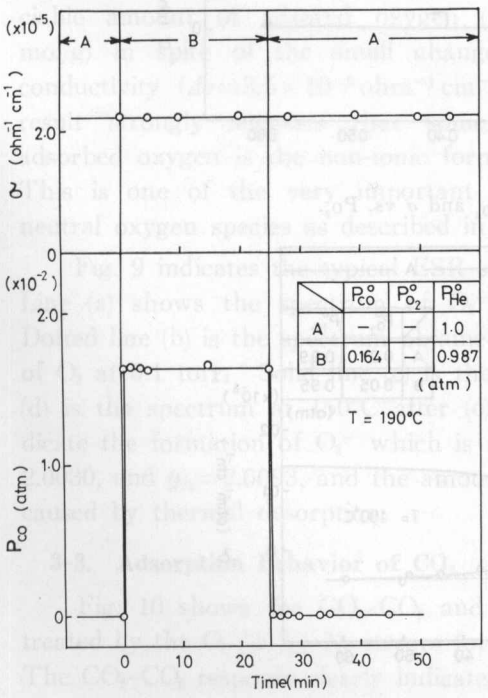

Fig. 5. The CO-CO and CO-σ responses.

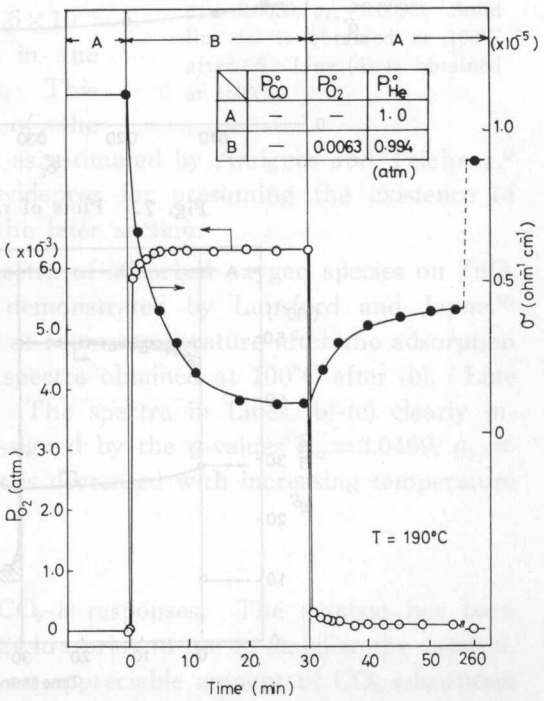

Fig. 6. The O_2-O_2 and O_2-σ responses.

response), shows a very slow decay of more than 200 min similar to the O_2 (inc., 0)-σ response. To explain this, two possibilities may be proposed: (1) O_2-flow caused by the impurity in the inlet He stream and (2) slow desorption of O_2 caused by its strong adsorption. The first possibility of (1) may be rejected, because the impurity involved is evaluated to be less than 50 ppm. In the present case one can recognize the amount more than 10^{-4} atm. (2) is thus reasonably accepted. As can be seen from the O_2 (dec., 0)-σ response, the steady state level (0.9×10^{-5} ohm^{-1} cm^{-1}) is lower than the previous steady state level (1.1×10^{-5} ohm^{-1} cm^{-1}). The strong adsorption of O_2 will mainly form O^- or O^{2-} rather than O_2^- based on the consideration of previous papers.[4,15] This also results from the strong adsorption of O_2 some of which is irreversibly adsorbed.

Fig. 7 illustrates the dependencies of the reaction rate and σ as a function of P_{O_2}. The steady state rate is zero order with respect to P_{O_2} whereas σ is

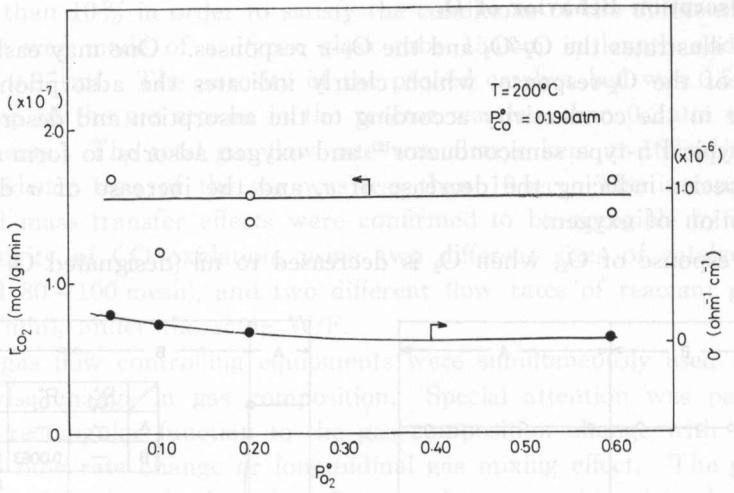

Fig. 7. Plots of r_{CO_2} and σ vs. P_{O_2}.

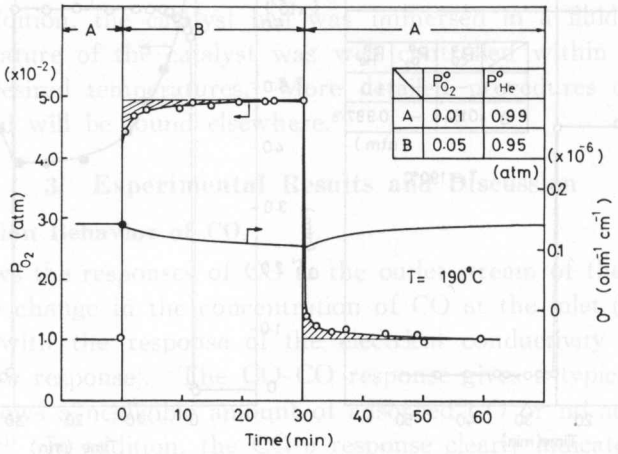

Fig. 8. The O_2-O_2 and the O_2-σ responses.

slightly decreased depending on P_{O_2}. Noting the absolute value of the conductivity change, the change is extremely small compared to those caused by the change in the concentration of CO, as $\Delta\sigma = 0.1 \times 10^{-6}$ ohm^{-1} cm^{-1} at $\Delta P_{O_2} = 0.2$ atm and $\Delta\sigma = 3.0 \times 10^{-6}$ ohm^{-1} cm^{-1} at $\Delta P_{CO} = 0.2$ atm which is one thirtieth (compare to Figs. 11 and 13). This results from the small change in the amount of charged oxygen species. From this result, one may recognize that the amount of charged oxygen species is not appreciably varied during the reaction by changing the concentration of O_2. The charged oxygen species contributing the slight increase of σ would be less active for CO oxidation. Based on Tanaka and Blyholder's conclusions,[1~4] the less active charged oxygen species may be O_2^-. H. Chon and J. Pajares[16] estimated 100% of the adsorbed oxygen to be O_2^- up to 180°C and 100% O^- higher than 230°C.

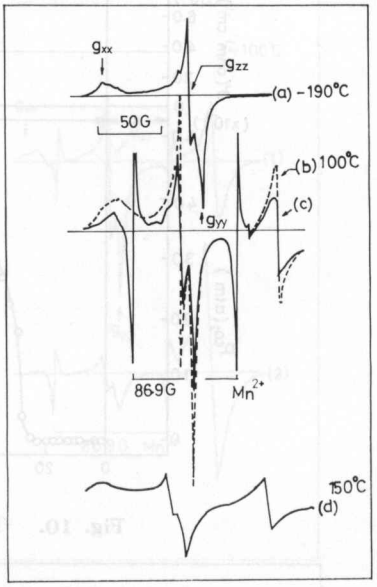

Fig. 9. ESR spectra of ZnO; Line (a) is referred from Lunsford et al ($g_{xx} = 2.0510$, $g_{yy} = 2.0020$, $g_{zz} = 2.0082$). Dotted line (b) is obtained at room temperature and $P_{O2} = 10$ torr. ($g_{xx} = 2.0499$, $g_{yy} = 2.0030$, $g_{zz} = 2.0093$). Solid line (c) is obtained at 100°C after (2). Line (d) is obtained at 150°C.

Fig. 8 shows the O_2-O_2 and O_2-σ responses. The former response, clearly indicates an appreciable amount of adsored oxygen (1.6×10^{-6} mol/g) in spite of the small change in the conductivity ($\Delta\sigma = 3.5 \times 10^{-8}$ ohm^{-1} cm^{-1}). This result strongly suggests that some of the adsorbed oxygen is the non-ionic form as estimated by Amigues and Teichner.[5] This is one of the very important evidences for presuming the existence of neutral oxygen species as described in the later section.

Fig. 9 indicates the typical ESR spectra of adsorbed oxygen species on ZnO. Line (a) shows the spectrum of O_2^- demonstrated by Lunsford and Jayne.[17] Dotted line (b) is the spectrum obtained at room temperature after the adsorption of O_2 at 0.1 torr. Solid line (c) is the spectra obtained at 100°C after (b). Line (d) is the spectrum at 150°C after (c). The spectra in Lines (b)-(c) clearly indicate the formation of O_2^- which is assigned by the g-values $g_{xx} = 2.0499$, $g_{yy} = 2.0030$, and $g_{zz} = 2.0093$, and the amount is decreased with increasing temperature caused by thermal desorption.

3-3. Adsorption Behavior of CO_2

Fig. 10 shows the CO_2-CO_2 and CO_2-σ responses. The catalyst has been treated by the O_2 (20%)-N_2 stream for 24 hrs prior to use to stabilize the catalyst. The CO_2-CO_2 response clearly indicates an appreciable amount of CO_2 adsorption whereas no change in the conductivity of the catalyst is observed. One may

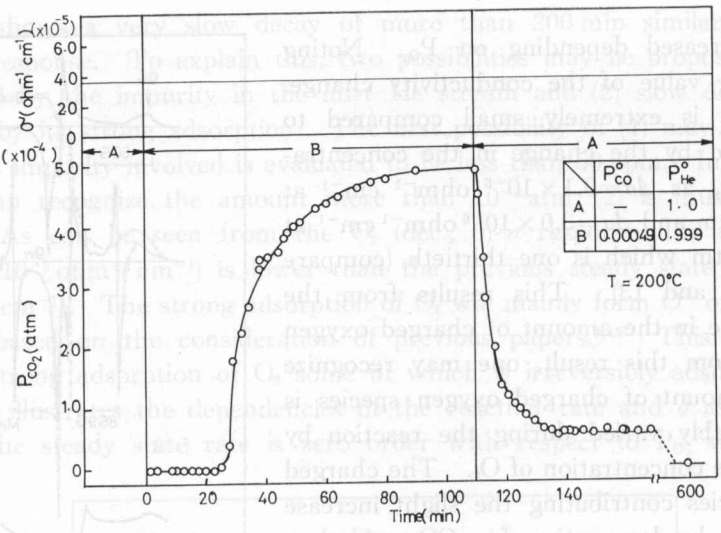

Fig. 10. The CO_2–CO_2 and CO_2–σ responses.

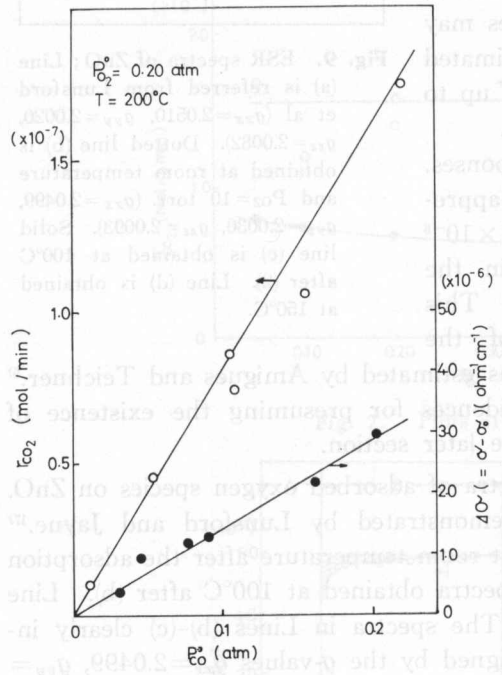

Fig. 11. Plots of σ and r_{CO_2} vs, Pco.

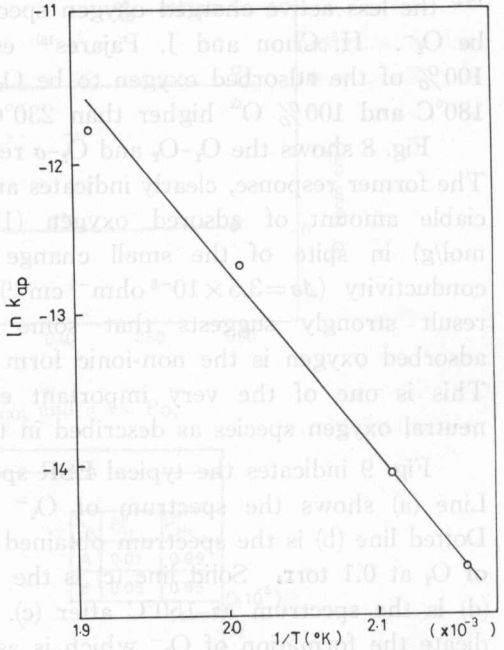

Fig. 12. Arrhenius plots of the apparent rate constant k_{ap}.

recognize CO_2 to be adsorbed with no charge transfer to the catalyst.

3-4. Transient Behavior of Oxygen Species in the Oxidation of CO

As described in the previous section, the steady state rate is zero order on the concentration of O_2. Fig. 11 illustrates the apparent first order kinetics in the concentration of CO. The Arrhenius plots of the apparent rate constant are

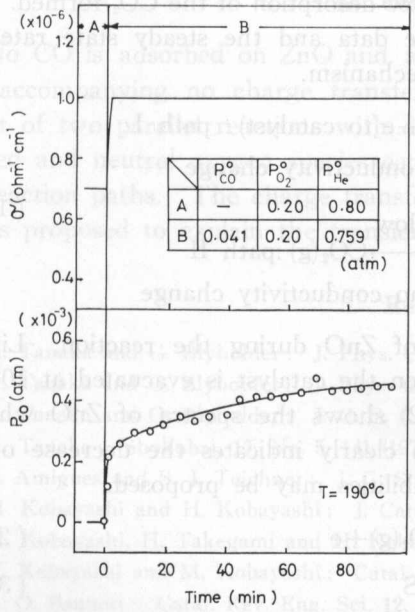

Fig. 13. The CO (inc, 0)-CO_2 and the CO (inc, 0)-σ responses.

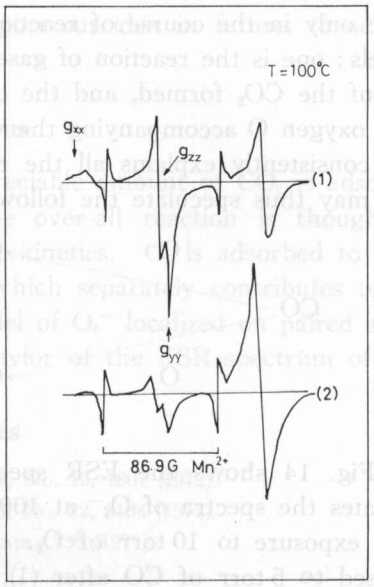

Fig. 14. ESR derivative spectra of oxygen adsorbed on ZnO. Exposure at 100°C.

Line (1) is observed at $P_{O_2}=0.1$ torr and 100°C. Line (2) is observed at the addition of CO ($P_{CO}=5$ torr) after (1).

shown in Fig. 12, evaluating 104 kJ/mol of apparent activation energy. From these results, it seems that the reaction is controlled by the surface reaction between adsorbed active oxygen and gaseous CO (or weakly adsorbed CO) with no appreciable inhibition effect of CO_2-adsorption on the reaction.

Fig. 13 illustrates the CO-CO_2 and the CO-σ responses. The CO(inc., 0)-CO_2 response consists of two parts: one is the instantaneous response and the other is the slow increase response over one hundred minutes. Based on the classification of the mode of transient response curves, this characteristic mode belongs to a typical type VI mechanism with two different reaction paths I and II.[11] The rate determining step of the reaction path I is the surface reaction of CO with adsorbed oxygen (corresponding to the rapid increase part of the curve), and path II will be controlled by both the surface reaction and the desorption of CO_2 (corresponding to the extraordinarily slow increase of the curve). One may recognize the slow desorption of CO_2 in path II from the mode of the very slow decay of the CO (dec., 0)-CO_2 response. Since the population of path II in the total over-all reaction is small, (less than 20% at 225°C), it is not large enough to cause the deviation of the total reaction rate from first order kinetics.

On the CO-σ response in Fig. 13, the conductivity change shows a characteristic instantaneous response which is very similar to the change in the rate of reaction path I. This similarity leads to the conclusion that the σ-change will

occur only in the course of reaction path I. One may presume two Eley-Rideal models : one is the reaction of gaseous CO and O^- followed by the rapid desorption of the CO_2 formed, and the other is the reaction of gaseous CO and non-ionic oxygen O accompanying the very slow desorption of the CO_2 formed. This idea consistently explains all the response data and the steady state rate data. One may thus speculate the following mechanism.

$$\mathrm{CO}\begin{cases}\xrightarrow{\mathrm{O^-}} \mathrm{CO_2(g)+e(to\ catalyst)}: \text{path I} \\ \qquad\qquad \text{conductivity change} \\ \xrightarrow[\text{slow}]{\mathrm{O}} \mathrm{CO_2\cdot S\longrightarrow CO_2(g)}: \text{path II} \\ \qquad\qquad \text{no conductivity change}\end{cases} \tag{1}$$

Fig. 14 shows the ESR spectrum of ZnO during the reaction. Line (1) indicates the spectra of O_2^- at 100°C when the catalyst is evacuated at 10^{-3} torr after exposure to 10 torr of O_2. Line (2) shows the spectra of ZnO which is exposed to 5 torr of CO after (1), which clearly indicates the decrease of O_2^-. To explain this result the following possibilities may be proposed.

$$\text{(i)}\quad \mathrm{O_2^-\cdot S+CO(g)\longrightarrow CO\cdot S+O_2(g)+e} \tag{2}$$

$$\text{(ii)}\quad \mathrm{O^-\cdot S+CO(g)\longrightarrow CO_2+e+S} \tag{3}$$

$$\mathrm{O_2^-\cdot S+e+S\longrightarrow 2O^-\cdot S} \tag{4}$$

$$\text{(iii)}\quad \mathrm{O^-\cdot S_1+(O_2{}^-{*}S_2+S_1)+CO(g)\longrightarrow CO_2(g)+O_2\cdot S_2+(2e+2S_1)} \tag{5}$$

$$\mathrm{O_2(g)+(2S_1+2e)\longrightarrow 2O^-\cdot S_1} \tag{6}$$

$$\mathrm{O_2\cdot S_2+e\longrightarrow O_2^-\cdot S_2} \tag{7}$$

$$\text{(iv)}\quad \mathrm{O_2^-\cdot S+CO(g)\longrightarrow CO_2(g)+O^-\cdot S} \tag{8}$$

where $(2e+2S_1)$ is the localized electron on the paired sites.

Since the separate experiments found no replacement of O_2^- due to the adsorption of CO, possibility (i) is rejected. (ii) and (iv) may also be rejected because of Tanaka and Blyholder's conclusions.[1~4] In this study, (iii) finally explains the charge transfer from site S_2 to S_1 according to the addition of CO. Tanaka and Blyholder did not consider this possibility. In our case, the intensity of the ESR spectrum of O_2^- is easily decreased depending on heating and the addition of CO. Although there is no evidence to support the activity of O_2^- differing from Tanaka et al's conclusions, based on our results. one may presume the possibility of the electron transfer from site S_2 to S_1. One may speculate that two paired vacant sites and electrons are necessary to form O^- according to equation (6). O_2^- thus indirectly helps to form O^- which is active for CO oxidation (see equation (5)). For a physical image of the active site, the coordinatively unsaturated surface ions on corners and other defects may be considered. It is

necessary to gather more detailed data to support our idea in future, to achieve more concrete conclusions.

4. Conclusions

No CO is adsorbed on ZnO and an appreciable amount of CO_2 is adsorbed with accompanying no charge transfer. The over-all reaction is thought to consist of two parallel reactions with different kinetics. O_2 is adsorbed to form charged and neutral oxygen species each of which separately contributes to the two reaction paths. The charge transfer model of O_2^- localized on paired active sites is proposed to explain the transient behavior of the ESR spectrum of O_2^-.

5. References

1) K. Tanaka and G. Blyholder: J. Phys. Chem., **76**, No. 13, 1807 (1972).
2) K. Tanaka and G. Blyholder: J. Phys. Chem., **76**, No. 22, 3184 (1972).
3) K. Tanaka and G. Blyholder: J. C. S. Chm. Comm., 736 (1971).
4) K. Tanaka: Shokubai, **17**, No. 5, 141 (1975).
5) P. Amigues and S. J. Teichner: J. C. S. Faraday Trans. 1, **63**, 362 (1967).
6) M. Kobayashi and H. Kobayashi: J. Catal., **27**, 100 (1984).
7) M. Kobayashi, H. Takegami and H. Kobayashi: J. C. S. Chem. Comm., **37** (1977).
8) H. Kobayashi and M. Kobayashi: Catal. Rev. Eng. Sci., S10, 104 (1974).
9) C. O. Bennett: Catal. Rev. Eng. Sci, **12**, 105 (1976).
10) M. Kobayashi: Chm. Eng. Sci., **37**, 393 (1982).
11) F. F. Volkenshtein: "The Electronic Theory of Catalysis on Semiconductors" Pergamon Press, (1963).
12) A. A. Tsyganenko: L. A. Denisenko, S. M. Zverev and V. N. Filimonov, J. Catal., **94**, 10 (1985).
13) A. B. Anderson and J. A. Nichols: J. Am. Chm. Soc., **108**, 1385 (1986).
14) H. Horiguchi, M. Setaka, K. M. Sacier and T. Kwan: Proceedings of the 4th. Intl. Cong. Catal., Moscow, 1968.
15) H. Chon and J. Pajares, J. Catal., **14**, 257 (1969).
16) J. M. Lunsford and J. P. Jayne: J. Chm. Phys., **44**, No. 4, 1487 (1966).